Harju, A.; Siljamäki, S.; Nieminen, R.M.

Two-electron quantum dot molecule: Composite particles and the spin phase diagram

Published in:
Physical Review Letters

DOI:
10.1103/PhysRevLett.88.226804

Published: 01/01/2002

Document Version
Publisher's PDF, also known as Version of record

Please cite the original version:
Harju, A., Siljamäki, S., & Nieminen, R. M. (2002). Two-electron quantum dot molecule: Composite particles and the spin phase diagram. *Physical Review Letters*, *88*(22), 1-4. [226804].
https://doi.org/10.1103/PhysRevLett.88.226804

Two-Electron Quantum Dot Molecule: Composite Particles and the Spin Phase Diagram

A. Harju, S. Siljamäki, and R. M. Nieminen
Laboratory of Physics, Helsinki University of Technology, P.O. Box 1100, 02015 HUT, Finland
(Received 7 January 2002; published 20 May 2002)

We study a two-electron quantum dot molecule in a magnetic field by the direct diagonalization of the Hamiltonian matrix. The ground states of the molecule with the total spin $S = 0$ and $S = 1$ provide a possible realization for a qubit of a quantum computer. Switching between the states is best achieved by changing the magnetic field. Based on an analysis of the wave function, we show that the system consists of composite particles formed by an electron and flux quanta attached to it. This picture can also be used to explain the spin phase diagram.

DOI: 10.1103/PhysRevLett.88.226804 PACS numbers: 73.21.La, 71.10.–w

The progress in semiconductor technology has opened a rich field of studies focused on the fundamental electron-electron interactions and quantum effects in artificial atoms and molecules [1]. The most striking feature of two-dimensional semiconductor quantum dots (QD) and quantum dot molecules (QDM) is that the correlation and magnetic field effects are greatly enhanced compared with their normal counterparts. This results in a rich variety of phenomena in lateral QDMs that have recently been investigated experimentally and theoretically; see, for example, Refs. [2–8]. Also the system parameters can easily be changed, unlike in real atoms and molecules where the parameters are natural constants. The controllable parameters make it possible to tailor the semiconductor structures and, for example, to switch between different ground states.

In this Letter we concentrate on a two-electron QDM consisting of two laterally coupled QDs. It has previously been studied, for example, in Refs. [6–9], but unlike these studies, we treat the electron correlations accurately. Our results show that these correlation effects are significant, as they result in new physical phenomena not seen in the previous works. An example of our interesting findings is that the system naturally consists of composite particles of electrons and flux quanta as in the composite-fermion theory [10].

In addition to the interesting and fundamental correlation and quantum effects, this system is very important as a candidate for the gate of a quantum computer [7,8]. A central idea is to use the total spin (S) of the two-electron QDM as a qubit. The ground state spin of the QDM can be either $S = 0$ or $S = 1$. One of the aims of this Letter is to study the regions of $S = 0$ and $S = 1$ states as a function of the important system parameters in their realistic range, beyond the approximations of Refs. [7,8] where a change in S was found when the magnetic field B was varied. We find a similar crossing at weak B, but also a reappearance of the $S = 0$ ground state at larger B. This is caused by the correlation effects that are treated accurately in our many-body approach.

We model the two-electron QDM by a 2D Hamiltonian

$$H = \sum_{i=1}^{2} \left(\frac{(-i\hbar\nabla_i - \frac{e}{c}\mathbf{A})^2}{2m^*} + V_c(\mathbf{r}_i) \right) + \frac{e^2}{\epsilon r_{12}}, \quad (1)$$

where V_c is the external confining potential, for which we use the one of Ref. [6], namely, $\frac{1}{2}m^*\omega_0^2 \min\{(x - d/2)^2 + y^2, (x + d/2)^2 + y^2\}$. This potential separates to two QDs at large interdot distances d, and with $d = 0$ it simplifies to one parabolic QD. We use GaAs material parameters $m^*/m_e = 0.067$ and $\epsilon = 12.4$, and the confinement strength $\hbar\omega_0 = 3.0$ meV. $\mathbf{A}$ is the vector potential of the magnetic field (along the z axis) taken in the symmetric gauge. One should note that the Hamiltonian is spin-free, and the Zeeman coupling $E_Z = g^*\mu_B B S_z$ (with $g^* = -0.44$ for GaAs) of the magnetic field to S_z can be taken into account afterwards. The eigenstates of the single-particle part of Eq. (1) are easily obtained as expansions

$$\psi(\mathbf{r}) = \sum_i \alpha_i \phi_i(\mathbf{r}) = \sum_i \alpha_i x^{n_{x,i}} y^{n_{y,i}} e^{-r^2/2}, \quad (2)$$

where n_x and n_y are integers and α_i is a complex coefficient. We have used the unit of length as in Ref. [11]. Figure 1 shows examples of the noninteracting charge densities, and Fig. 2 displays single-particle energies.

It is interesting to compare the localizing effect of B with the experimental findings of Brodsky *et al.* [3]. They see a clear splitting of the QDM electron droplet to smaller fragments by a strong B. As they work in a low-density limit (weak confinement), impurities can have a similar role as the potential minima in Fig. 1. The localization is also related to the formation of Wigner molecules in QDs [11], which happens in the low-density limit.

Similarly to the single-particle states, the full many-body wave function with total spin S can be expanded as

$$\Psi_S(\mathbf{r}_1, \mathbf{r}_2) = \sum_{i \le j} \alpha_{i,j} \{ \phi_i(\mathbf{r}_1)\phi_j(\mathbf{r}_2) + (-1)^S \phi_i(\mathbf{r}_2)\phi_j(\mathbf{r}_1) \}, \quad (3)$$

which is symmetric for $S = 0$ and antisymmetric for $S = 1$. Notice that the spin part of the wave function is not

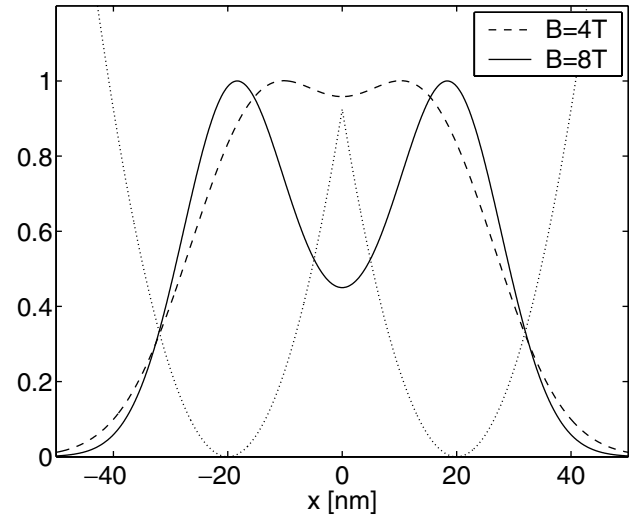

FIG. 1. Confinement potential V_c (dotted line) and noninteracting single-particle density $|\psi|^2$ along $y = 0$ for $d = 40$ nm. The potential is in units of $\hbar\omega_0 = 3$ meV, and the maximum value of each $|\psi|^2$ is scaled to unity. The confinement potential is parabolic in the y direction. One can see a localizing effect of large d and strong B.

explicitly written, and we work with spin-independent wave functions also below. The coefficient vector $\boldsymbol{\alpha}_l$ and the corresponding energy E_l for the lth eigenstate are found from a generalized eigenvalue problem where the Hamiltonian and overlap matrix elements can be calculated analytically. Details of the computational procedure will be published elsewhere [12]. As the basis functions we have used all the states with both n_x and $n_y \leq n$ with $n = 6$, and we have checked the convergence by varying n for all values of d.

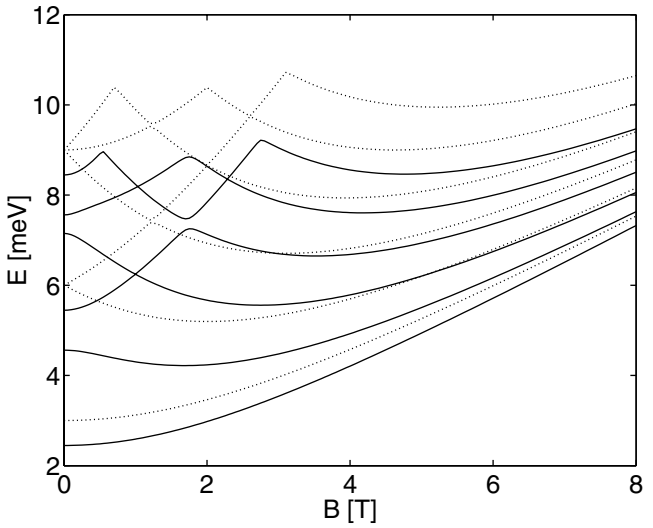

FIG. 2. Six lowest noninteracting single-particle energies as a function of B. The dotted lines are the normal Fock-Darwin states ($d = 0$), and the solid ones are for $d = 20$ nm. One can see that for $d > 0$, the energies are shifted down and that the level crossings occur at weaker B. At some of the level crossings a gap opens, such as the one for $B \approx 1.75$ T, $E \approx 7.4$ meV. This is due to the lower symmetry of the problem for $d > 0$. In general, there is a reasonable similarity between the two sets of energy levels. For sufficiently large d, the energies would converge to degenerate states of isolated dots. All states are on the lowest Landau level after $B \approx 3$ T.

The energy difference ΔE between the lowest $S = 1$ and $S = 0$ states is plotted in Figs. 3 and 4. The convergence of ΔE can be seen in Fig. 4 for large d. One can see that for weak magnetic field values, the ground state has $S = 0$. We first concentrate on this regime. For $B = 0$ the $S = 0$ state remains lower with arbitrary d, see, e.g., Ref. [6] for a discussion of this exact property. However, there is a strong decrease in ΔE as a function of d. This can be understood from the fact that very distant QDs interact only weakly and the energy difference of the two spin states is smaller. There is also a strong decrease in ΔE as a function of B in the $S = 0$ state. For $d = 0$, ΔE is rather linear until the crossing to the $S = 1$ state, but for $d > 0$ the curves are rounded. The crossing point of the different ground states does not depend strongly on d; it changes only from 1.6 to 1.2 T as one moves from $d = 0$ to 40 nm. Because of this, changing the total spin in an experimental setup is not easy by just changing d. On the other hand, around $\Delta E = 0$, the slope of ΔE is rather large and changing S by B is the most natural choice. One can achieve a change of S also by changing the strength of V_c. This changes the ratio between the energies resulting from the confinement and electron-electron interaction. For a weak V_c, the interactions are stronger and the transition occurs at weaker B value. Thus the change of the V_c can be seen as a change of the effective value of B.

The transition from the weak-B $S = 0$ state to the $S = 1$ state is most simply explained by the fact that the energies of the two lowest single-particle states approach each other as B is made stronger (see Fig. 2). At some point this difference is smaller than the exchange energy, and

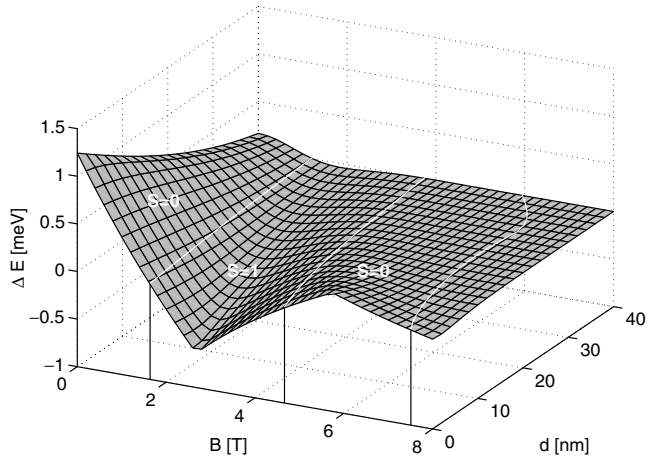

FIG. 3. Energy difference between triplet and singlet states ΔE as a function of the magnetic field B and interdot separation d. The white lines separate the $S = 0$ ($\Delta E > 0$) and $S = 1$ ground states.

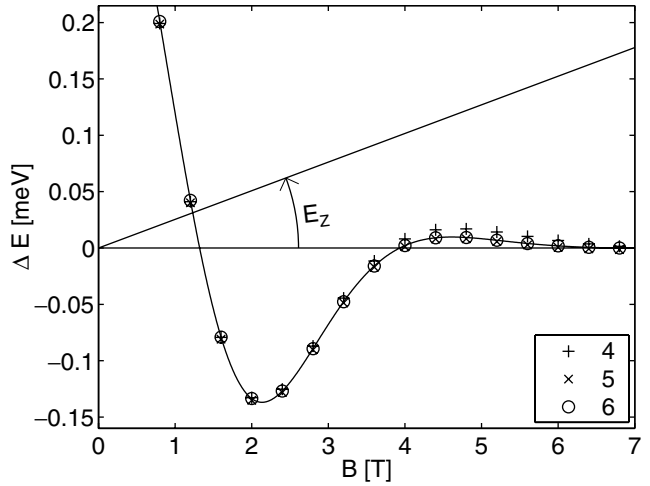

FIG. 4. ΔE for a fixed $d = 26.736$ nm [13]. The effect of the Zeeman energy E_Z is also shown. The difference between expansions with $n = 5$ and 6 is only around 1 μeV. One can see that the second $S = 0$ state disappears for even a weak E_Z.

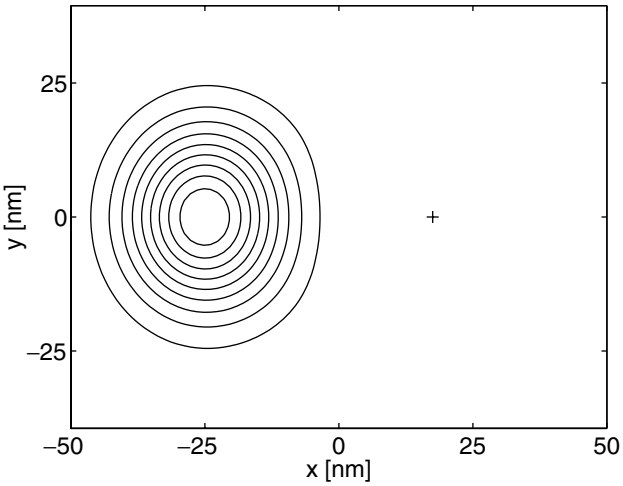

FIG. 5. $|\Psi[(x, y), (d/2, 0)]|^2$ for the state $S = 0$ at $B = 4.5$ T and $d = 35$ nm. The contour spacing is uniform. We mark with a plus the fixed electron on the right-hand QD. One can see that the electron density is localized to the left QD. There is only a small deformation from circular symmetry. Notice that the effective interdot distance is much larger than d due to the Coulomb repulsion of the electrons.

the system spin-polarizes. One can see that also for this state, ΔE decreases strongly as a function of d.

There exists a second region of $S = 0$ ground state around $B \approx 6$ T at $d = 0$. The question whether this state terminates at large d remains open, as the energy differences at $d > 40$ nm are smaller than the error made in the expansion. The existence of this $S = 0$ state for a small value of d can be understood on the basis of a parabolic two-electron QD, which can be shown to have the exact wave function of the form $\Psi = (x_{12} + iy_{12})^m f(r_{12}) e^{-(r_1^2 + r_2^2)/2}$, where m is the relative angular momentum and f is a correlation factor [14]. The simple form is due to the separation of the center of mass and relative motion of the electrons. For $B = 0$ the ground state has $m = 0$ (and $S = 0$), and when B is made stronger, the ground state m has increasing positive integer values. These transitions happen because the larger m states have smaller Coulomb repulsion between the electrons, and as the single-particle energies group together to form the lowest Landau level, it is favorable to move to larger m. The second $S = 0$ region in Fig. 3 corresponds to $m = 2$. It is surprising that the second $S = 0$ region extends to such a large d. For example, at $B = 4.5$ T and $d = 35$ nm the two QDs of a QDM are rather decoupled (see Fig. 5), but still the $S = 0$ state remains the ground state. To analyze the structure of this state for small and large values of d, we have located the vortices of Ψ. This can be done by finding the zeros of Ψ and studying the change in the phase of Ψ in going around each of the zeros. A surprising finding is that for both large d and $d = 0$ there are two vortices at both electron locations; see Fig. 6 for an example. The particles are thus composite particles of an electron and two flux quanta, in similar fashion as in the composite fermion (CF) theory [15]. The most remarkable feature of the finding is the stability of composite particles against the change of d.

We have done a similar analysis for the $S = 1$ state at $B = 3$ T and various values of d. We found that the many-body state again consists of composite particles, but this time there is only one flux quantum per electron. One should note that for an odd number of flux quanta per electron, the wave function changes sign when the particles are exchanged, corresponding to $S = 1$. Similarly, for even flux numbers the state has $S = 0$.

If one expands $|\Psi|^2$ for small r_{12}, one obtains

$$|\Psi|^2 \propto r_{12}^{2m} + \frac{C}{m + \frac{1}{2}} r_{12}^{2m+1} + \mathcal{O}(r_{12}^{2m+2}), \qquad (4)$$

where C is the scaled strength of the Coulomb interaction [11], and $m \geq 0$ is the number of flux quanta per electron. One can see that for larger m values, the density grows more slowly as a function of r_{12} (see Fig. 6). One should

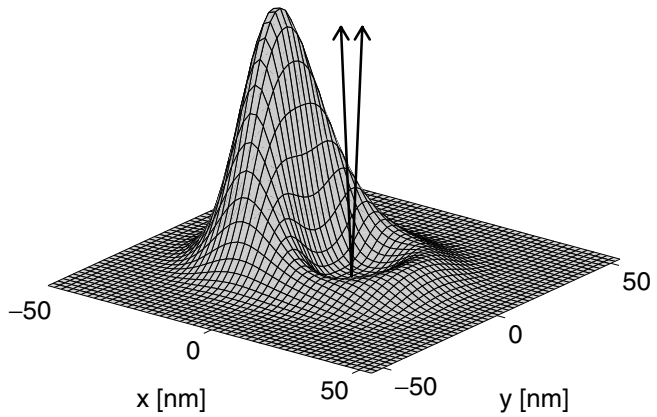

FIG. 6. $|\Psi[(x, y), (d/2, 0)]|^2$ for the state $S = 0$ at $B = 6$ T and $d = 10$ nm. The arrows (rotated for clarity) depict the two flux quanta at the electron fixed at $x > 0$ minimum of V_c.

note that the same expansion is valid also for the larger electron numbers, resulting from the cusp condition [11]. Thus the electron-electron interaction is smaller when the number of flux quanta per electron grows.

One can use the CF-type approach to explain the phase diagram of Fig. 3. When one moves from $B = 0$ to stronger values of B, the number of flux quanta in the system increases. At the first $S = 0$ state there are no fluxes in the system, and at the transition point the flux number changes to one per electron. For weakly coupled QDs this transition happens at smaller B than in the strongly coupled ones, because a distant zero of the wave function increases the kinetic energy less than a close one does. In the following transition points the number of flux quanta changes again by one per electron. The reasoning for the d dependence of the first transition applies to other ones also, and this can be seen in Fig. 3.

An interesting prospect resulting from the discussion above is to use the CF-type approach to describe the many-body states of electrons at strong B in various confining potentials. One should note that after the phase structure of the wave function is fixed, one is left with the bosonic part of the wave function. The quantum Monte Carlo techniques are especially useful for obtaining this part [16].

If one adds the Zeeman term to the Hamiltonian, the energy of the $S = 1$ state is lowered by $\sim 25\ \mu\mathrm{eV/T}$ and the $S = 0$ energy is unaltered; see Fig. 4. This makes the high-B $S = 0$ state to terminate at d value around 5 nm. One should note that it is possible to lower the Zeeman term also in the experimental setup by applying a tilted magnetic field. Most probably the singlet-triplet separation in energy for $B \approx 6$ T is too small for a qubit, but, in principle, it is possible to change S by varying the Zeeman term in this parameter range.

In conclusion, we have determined the total-spin phase diagram of the two-electron quantum dot molecule as a function of the magnetic field and the interdot distance. Our results support the possibility to use the system for a gate of a quantum computer [7]. In addition, we have found that the system consists of composite particles of electrons and the attached magnetic field flux quanta.

This research has been supported by the Academy of Finland through its Centers of Excellence Program (2000–2005).

[1] R. C. Ashoori, Nature (London) **379**, 413 (1996).
[2] T. H. Oosterkamp, S. F. Godijn, M. J. Uilenreef, Y. V. Nazarov, N. C. van der Vaart, and L. P. Kouwenhoven, Phys. Rev. Lett. **80**, 4951 (1998).
[3] M. Brodsky, N. B. Zhitenev, R. C. Ashoori, L. N. Pfeiffer, and K. W. West, Phys. Rev. Lett. **85**, 2356 (2000).
[4] T. H. Oosterkamp, T. Fujisawa, W. G. van der Wiel, K. Ishibashi, R. V. Hijman, S. Tarucha, and L. P. Kouwenhoven, Nature (London) **395**, 873 (1998).
[5] C. Yannouleas and U. Landman, Phys. Rev. Lett. **82**, 5325 (1999); S. Nagaraja, J.-P. Leburton, and R. M. Martin, Phys. Rev. B **60**, 8759 (1999).
[6] A. Wensauer, O. Steffens, M. Suhrke, and U. Rössler, Phys. Rev. B **62**, 2605 (2000).
[7] G. Burkard, D. Loss, and D. P. DiVincenzo, Phys. Rev. B **59**, 2070 (1999).
[8] X. Hu and S. Das Sarma, Phys. Rev. A **61**, 062301 (2000).
[9] C. Yannouleas and U. Landman, Eur. Phys. J. D **16**, 373 (2001); see also e-print cond-mat/0109167.
[10] J. K. Jain, Phys. Today **53**, No. 4, 39 (2000).
[11] A. Harju, S. Siljamäki, and R. M. Nieminen, Phys. Rev. B **65**, 075309 (2002).
[12] A. Harju, S. Siljamäki, and R. M. Nieminen (unpublished).
[13] Density-functional theory finds the first transition to $S = 1$ at $B \approx 1.25$ T; see H. Saarikoski, E. Räsänen, S. Siljamäki, A. Harju, M. J. Puska, and R. M. Nieminen, Eur. Phys. J. B **26**, 241 (2002).
[14] A. Harju, B. Barbiellini, R. M. Nieminen, and V. A. Sverdlov, Physica (Amsterdam) **255B**, 145 (1998).
[15] J. K. Jain and T. Kawamura, Europhys. Lett. **29**, 321 (1995).
[16] G. Ortiz, D. M. Ceperley, and R. M. Martin, Phys. Rev. Lett. **71**, 2777 (1993).